Electrostatic Domino Effect in the *Shaker* K Channel Turret

Amir Broomand,* Fredrik Österberg,* Tara Wardi,[†] and Fredrik Elinder*
*Department of Biomedicine and Surgery, Division of Cell Biology, Linköpings Universitet, Linköping, Sweden;
and [†]Department of Neuroscience, Karolinska Institutet, Stockholm, Sweden

ABSTRACT   Voltage-gated K channels are regulated by extracellular divalent cations such as Mg^{2+} and Sr^{2+}, either by screening of fixed negative surface charges, by binding directly or close to the voltage sensor, or by binding to the pore. Different K channels display different sensitivity to divalent cations. For instance, 20 mM $MgCl_2$ shifts the conductance versus voltage curve, $G(V)$, of the Kv1-type *Shaker* channel with 14 mV, while the $G(V)$ of Kv2.1 is shifted only with 7 mV. This shift difference is paralleled with different working ranges. Kv1-type channels open at ~ -20 mV and Kv2.1 channel open at $\sim +5$ mV. The aim of this study was to identify critical residues for this Mg^{2+}-induced $G(V)$ shift by introducing Kv2.1 channel residues in the *Shaker* K channel. The K channels were expressed in *Xenopus laevis* oocytes and studied with the two-electrode voltage-clamp technique. We found that three neutral-to-positive amino-acid residue exchanges in the extracellular loops connecting transmembrane segments S5 and S6 transferred the Mg^{2+}-shifting properties. The contributions of the three residues were additive, and thus independent of each other, with the contributions in the order 425 > 419 > 451. Charging 425 and 419 not only affect the Mg^{2+}-induced $G(V)$ shift with 5–6 mV, but also shifts the $G(V)$ with 17 mV. Thus, a few strategically placed surface charges clearly modulate the channel's working range. Residue 425, located at some distance away from the voltage sensor, was shown to electrostatically affect residue K427, which in turn affects the voltage sensor S4—thus, an electrostatic domino effect.

INTRODUCTION

Opening and closing of voltage-gated ion channels underlies the generation of nerve and muscle action potentials, synaptic transmission, and hormone secretion. These channels open in response to a change in the membrane electric field, allowing ions to pass through the channel pore and generating an electrical current. In addition to being selectively conductive to specific ions, the channels are also regulated by divalent cations (1). Frankenhaeuser and Hodgkin (2) showed that Ca^{2+} and Mg^{2+} affect voltage-gated Na^+ and K^+ channels by shifting the voltage-dependent parameters of the ion channels along the voltage axis. That is, an increase of divalent cations on the extracellular side of the nerve membrane required more positive voltage steps to open the channel. It has been suggested that some divalent cations (e.g., Mg^{2+} and Sr^{2+}) mainly screen fixed negative surface charges, thereby changing the surface potential and consequently the local electric fields within the membrane. Other ions, such as Zn^{2+} and Cd^{2+}, mainly bind to specific sites on the channel, thereby changing the surface charge density (and consequently the surface potential) and the local electric fields within the membrane (1,3).

Altering the valence of a surface charge will alter the electric field sensed by the voltage sensor and, hence, shift the voltage-dependent parameters of the ion channel along the voltage axis (3–5). We have found that different channels expressed in a common expression system (*Xenopus* oocytes) have different sensitivity to Sr^{2+} with respect to

their voltage-shifting properties, suggesting that some of the important surface charges are located on the channel protein itself (6,7). The most sensitive channels were some Kv1-type channels (Kv1.1 and *Shaker*), where addition of 20 mM $SrCl_2$ or $MgCl_2$ to the extracellular solution shifted the conductance versus voltage curve, $G(V)$, with 13–14 mV. The least-sensitive noninactivating channel was Kv2.1, where 20 mM Sr^{2+} shifted $G(V)$ with 7 mV. This difference in Mg^{2+}- or Sr^{2+}-shifting potency is paralleled by a difference in working range of channel opening. Kv1-type channels open at voltages at ~ -20 mV, while Kv2.1 open at $\sim +5$ mV (6). Thus, the distinct surface charges screened by Mg^{2+} also profoundly regulate the channels' working range with respect to voltage. While the binding sites for Zn^{2+} and Cd^{2+} are known in some cases (8), the identity of the fixed surface charges for the screening is unclear (1).

The aim of this investigation was to identify critical surface-charge residues by converting a highly Mg^{2+} sensitive K channel (*Shaker*) to a less Mg^{2+}-sensitive channel (Kv2.1). In previous work we have suggested that the important residues are located in the extracellular loops S5-P, connecting the transmembrane segment 5 and the pore, and P-S6, connecting the pore and the transmembrane segment 6 (P-S6) (5,9). The sequences for these two loops for *Shaker* and Kv2.1 are shown in Fig. 1 *A*. Surprisingly, the two channels have the same net charge (-1) if we add up all charges in the sequences. This suggests that the specific positions of the charged residues in the loops are critical for the Mg^{2+}-shifting effects, rather than the net charge. Our hypothesis is that the important positions are those with an excess of negative charges in *Shaker* or an excess of positive charges in Kv2.1. Three positions fulfill these criteria: 419,

A


```
KcsA      51  ERGAPGAQLITYP- pore -PVTLW  87
Shaker   418  EAGSENSFFKSIP- pore -PVGFW 454

419C/425K/451K
         418  ECGSENSKFKSIP- pore -PKGFW 454
Kv2.1    353  EKDEDDTKFKSIP- pore -PKTLL 389
```
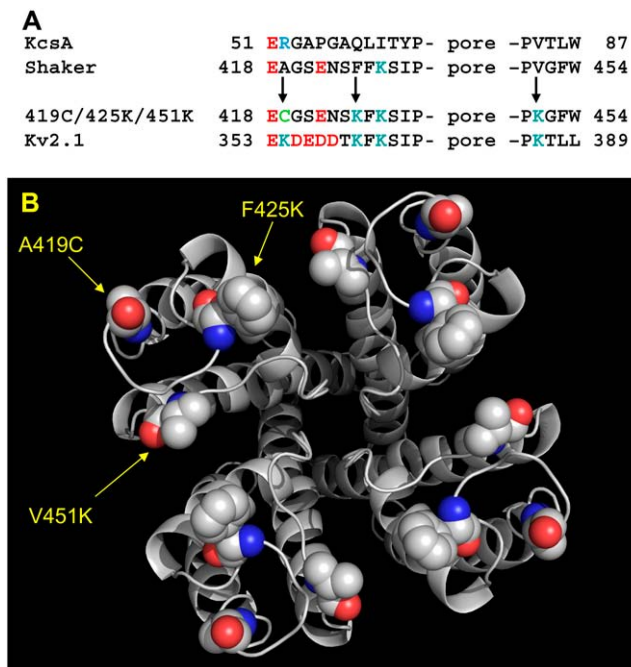
B

FIGURE 1   Positions of mutated residues. (*A*) The sequences of the loop amino acids between S5-P and P-S6 in KcsA, *Shaker*, A419C/F425K/V451K, and Kv2.1 channels. The triple mutation changes are shown by arrows. Negative charges in red, positive charges in blue, and cysteine in green. (*B*) Modeled *Shaker* channel from x-ray structure KcsA channel viewed from the extracellular side. Eight combinations of charged residues in positions 419, 425, and 451 were used.

425, and 451 are neutral in *Shaker* while the corresponding residues in Kv2.1 are positively charged. These three positions are mapped on the extracellular surface of the *Shaker* channel modeled from the x-ray structure of the KcsA channel (10) in Fig. 1 *B*.

By testing all combinations of positive charges in these three positions, we found that two of the residues contributed to the effect and that changing these two residues converted the *Shaker* channel to a Kv2.1 channel with respect to the voltage-shifting properties of Mg^{2+}.

MATERIALS AND METHODS

Molecular biology

The experiments were performed on *Shaker* H4 channels (11), made incapable of fast-inactivation by the Δ6–46 deletion (12). Cysteines were substituted using the QuikChange Kit (Stratagene, La Jolla, CA). cRNA was transcribed using the T7 mMessage mMachine kit (Ambion, Austin, TX) and injected in *Xenopus laevis* oocytes (20–500 pg/cell) using a Nanoject injector (Drummond Scientific, Broomall, PA). The oocytes were maintained in a modified Barth's solution (MBS, in mM: 88 NaCl, 1 KCl, 2.4 NaHCO$_3$, 15 HEPES, 0.33 Ca(NO$_3$)$_2$, 0.41 CaCl$_2$, and 0.82 MgSO$_4$) adjusted to pH 7.8 by NaOH, and supplemented with penicillin (10 μg/ml), streptomycin (10 μg/ml), and sodium pyruvate (10 μg/ml) . The electrophysiological experiments were made 3–5 days after injection of mRNA.

Electrophysiology, solutions, and reagents

The currents were measured with the two-electrode voltage-clamp technique (CA-1 amplifier, Dagan, Minneapolis, MN). Microelectrodes were made from borosilicate glass and filled with a 3 M KCl solution. The resulting resistance varied between 0.5 and 2.0 MΩ. The amplifier's capacitance and leak compensation were used, and the currents were low-pass-filtered at 5 kHz. All experiments were carried out at room temperature (20–23°C). For the electrophysiological experiments we used the 1 K solution (in mM: 88 NaCl, 15 HEPES, 1 KCl, 0.8 MgCl$_2$, and 0.4 mM CaCl$_2$) adjusted to pH 7.4 by NaOH. To screen surface charges, we added 20 mM MgCl$_2$ to the 1 K solution. Mg^{2+} ions have been shown to shift voltage-dependent parameters equally and, therefore, have been suggested to exert pure screening of surface charges without directly binding to K channels (1).

The simplest and most direct way to alter a charge of a residue is to apply charged cysteine-specific reagents that can modify a specifically inserted cysteine during the course of the experiment (e.g., (5,13)). Thus, the charge is changed in situ and the channel before modification can be used as its own control. This strategy gives more robust data with little interexperimental variability. To alter the charge at the substituted cysteine the membrane-impermeant thiol reagents, positively-charged (2-(trimethylammonium) ethyl) methanethiosulfonate bromide (MTSET; Toronto Research Chemicals, North York, Ontario, Canada) were applied continuously in the bath solution by a gravity-driven perfusion system, and the modification was assayed functionally in two-electrode voltage-clamped oocytes (see, e.g., Fig. 3 *B*). The cysteine reagent was applied to saturation (100 μM MTSET for 200 s). After modification, MTSET in the bath was carefully washed off. MTSET is a reagent that easily can build a sulfur-sulfur bridge with (for example) cysteine, and that has one positive charge. The modified and thus positively charged cysteine will be denoted C-ET$^+$. The modified residue is similar in structure and function to a native arginine or lysine, and thus this modification strategy should give results similar to changing a residue directly to a positively charged residue. In this investigation we changed the charge by making selected neutral residues positive. The reason for doing so was to convert the *Shaker* K channel to a Kv2.1 channel with respect to Mg^{2+}-shifting properties. The identified surface charge candidates are neutral in *Shaker* and positive in Kv2.1. From an electrostatic point of view, insertion of neutral MTS reagents should not affect the Mg^{2+}-shifting properties and negative MTS reagents should have opposite effects to the positive MTS reagent. This was shown to be the case when we studied several surface residues in a previous investigation (5).

Analysis

The steady-state K conductance $G_K(V)$ was calculated as

$$G_K(V) = I_K(V)/(V - E_K), \tag{1}$$

where $I_K(V)$ is the steady-state current, V is the membrane potential measured in the bulk solutions, and E_K is the equilibrium potential (−80 mV). The shifts of the $G(V)$ curves caused by either MTS reagents or Mg^{2+} were measured by sliding the control $G(V)$ to overlap (most importantly the lower part of the curves, since the curves were not normalized) the Mg^{2+} and/or MTS $G(V)$. The lower part of the curves best reflects the movement of the voltage sensor S4 of the channel. All data are given as mean ± SE.

Molecular dynamics

The x-ray structure of the bacterial channel KcsA (10) was used as a template structure for constructing a *Shaker*-like environment around residue F425. The important part in this work, the S5-linker to S6 helix, was altered to have the correct residue sequence of the *Shaker* K channel (Fig. 1 *A*). This was done by a simple replacement of KcsA residues with the program PyMOL (14).

Two molecular dynamic (MD) simulations were carried out by using the AMBER95 force field (15) with the program Q (16), one simulation with the *Shaker* channel as a wild-type with Phe in position 425 and one with Lys in the same position. Data collection was performed for a 500-ps run, after a stepwise heating of the system from 0 K to 300 K followed by a 25-ps equilibration of the system. A 34 Å sphere of explicit water were used in the MD simulations, centered just above position 1 in the selectivity filter, and a grid of nonpolar lipid atoms (17,18) were restrained to a three-dimensional grid with a force constant of 5 kcal mol^{-1} to avoid water molecules penetrating the membrane part of the potassium channel. The selectivity filter was filled with four water molecules restrained in the axial position by a force constant of 100 kcal mol^{-1} (17). Other parameters and settings were used as earlier (19,20).

RESULTS

In this article, we investigate the role of charged residues on the extracellular surface of the *Shaker* K channel for Mg^{2+}-induced $G(V)$ shifts (ΔV_{Mg}) along the voltage axis. Specifically, we focus on three positively charged residues: one at the extracellular end of S5 (A419), which has been suggested to be close to S4 (5,9,21,22), one at the extracellular end of the pore helix close to the pore (F425), and one at the extracellular end of S6 (V451). Fig. 1 *B* shows the location of these three residues in the modeled *Shaker* channel.

A triple neutral-to-positive charge mutation converts a highly Mg^{2+}-sensitive *Shaker* channel to a low Mg^{2+}-sensitive Kv2.1-like channel

Fig. 2 *A* shows the shift of the $G(V)$ curve when adding 20 mM Mg^{2+} to the *Shaker* WT K channel. The shift, ΔV_{Mg}, is 13.4 ± 0.3 mV (Table 1). To change the charge of a residue, we either mutated the residue to a positively charged lysine or we mutated a residue to a cysteine that was subsequently

modified to a positively charged residue with a covalently-linked cysteine-specific MTSET reagent (see Materials and Methods and the next section for a detailed description of the modification). The currents for the cysteine-modified triple mutant (A419C-ET$^+$/F425K/V451K) are WT-like (A. Broomand and F. Elinder, unpublished data) except that the $G(V)$ curve is shifted to a more positive voltage range ($V_{1/2} = -7.5 \pm 0.9$ mV versus $V_{1/2} = -24.5 \pm 1.0$ mV; Table 1). This shift most likely depends on a changed surface potential (three positive charges are added to each subunit) and hence changed local electric fields within the membrane (see Discussion).

Fig. 2 *B* shows the effect of Mg^{2+} on the $G(V)$ for the cysteine-modified triple mutant (A419C-ET$^+$/F425K/V451K). The average rightward shift along the voltage axis is 7.8 ± 0.3 mV, which is close to what we have reported for Kv2.1 (7.0 mV; (6)). Fig. 2 *C* shows a summary of the mean shifts for WT, for the single-neutral mutant A419C, and for the triple-positive mutant. Data from Kv2.1 is also shown as a comparison. Thus, the triple-positive mutation was able to convert the channel with high sensitivity to a channel with low sensitivity with respect to ΔV_{Mg}.

In the next step, we wanted to investigate the individual roles of the three different residues to the reduction in ΔV_{Mg}, and if the charges affected each other or not. To test this, we investigated the role of specific charge-reversal mutations in different channel backgrounds.

A charge at position A419C affects the voltage sensor independent of the channel background

In the first set of experiments, we investigated the role of a positive charge in position 419. The reason for selecting this
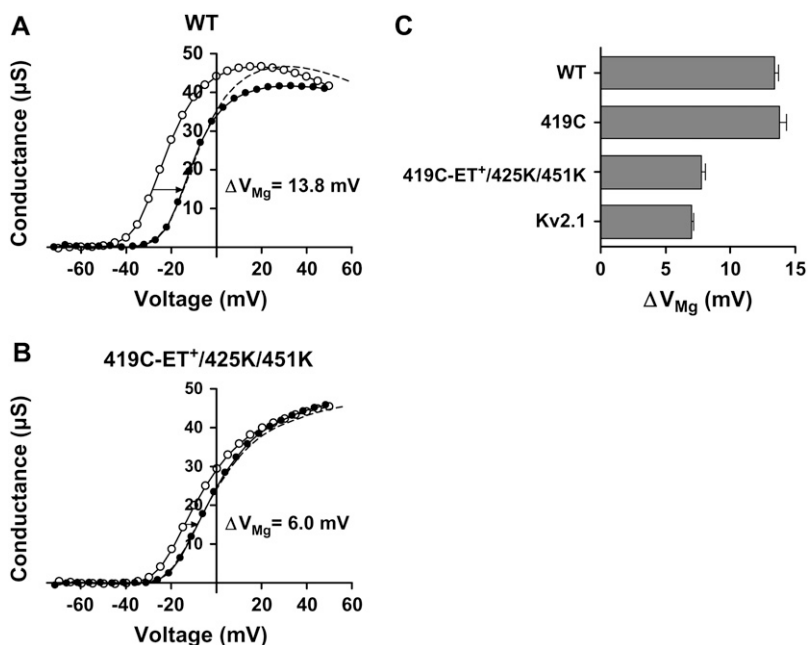

FIGURE 2 Mg^{2+}-induced $G(V)$ shifts. The conductance, $G(V)$, of the WT *Shaker* channel (*A*) compared to the conductance of the triple mutation (*B*). Control solution (○) and 20 mM Mg^{2+} solution (●). The dashed curves are the respective control curves moved along the *x* axis as indicated. (*C*) Summary of Mg^{2+}-induced shifts for four different channels. Data for Kv2.1 from Elinder et al. (6).

TABLE 1   Voltage-dependent parameters for channels with introduced positive charges

Channel	$V_{1/2}$ (mV)	$\Delta V_{1/2,MTSET}$	ΔV_{Mg} (mV)	$\Delta\Delta V_{Mg}$ (mV)
WT	−23.7 ± 2.2 (13)		13.4 ± 0.3 (11)	
A419C	−24.5 ± 1.0 (8)		13.8 ± 0.5 (13)	
A419C-ET[+]	−17.2 ± 3.4 (3)	6.1 ± 0.8 (6)***	11.7 ± 1.0 (6)	−2.0 ± 0.4 (5)**
A419C/F425K	−13.0 ± 1.0 (7)***		10.4 ± 0.5 (9)***	
A419C-ET[+]/F425K	−7.6 ± 0.9 (7)	5.4 ± 0.5 (7)***	8.5 ± 0.5 (9)	−1.9 ± 0.3 (9)***
A419C/V451K	−18.6 ± 1.2 (6)**		14.0 ± 0.5 (7)[ns]	
A419C-ET[+]/V451K	−14.3 ± 1.0 (6)	4.4 ± 0.8 (6)**	12.1 ± 0.6 (7)	−1.9 ± 0.3 (7)***
A419C/F425K/V451K	−11.7 ± 1.0 (5)***		10.0 ± 0.7 (5)***	
A419C-ET[+]/F425K/V451K	−7.5 ± 0.9 (5)	4.3 ± 0.2 (5)***	7.8 ± 0.3 (5)	−2.3 ± 0.4 (5)**
F425C/K427Q	−31.4 ± 1.1 (8)***		15.2 ± 0.6 (8)[ns]	
F425C-ET[+]/K427Q	−29.9 ± 1.7 (8)	1.5 ± 0.7 (8)[ns]	15.0 ± 0.5 (8)	−0.1 ± 0.2 (8)[ns]

$V_{1/2}$ is midpoint of the $G(V)$ curve, $\Delta V_{1/2,MTSET}$ is the MTSET induced $G(V)$ shift, ΔV_{Mg} is the Mg^{2+}-induced $G(V)$ shift, and $\Delta\Delta V_{Mg}$ is the MTSET-induced change in Mg^{2+}-induced $G(V)$ shifts. Two-tailed unpaired t-test between A419C and the other mutations ($V_{1/2}$, ΔV_{Mg}). Two-tailed, one sample t-test compared to 0 ($\Delta V_{1/2,MTSET}$, $\Delta\Delta V_{Mg}$). ns, not significant; *, $p < 0.05$; **, $p < 0.01$; and ***, $p < 0.001$.

charge is that it was the most sensitive position we found in an earlier study (5). Furthermore, to be able to get precise measurements, we changed the charge of the residue during the experiments by the use of cysteine-modifying reagents: A (neutral) cysteine was introduced at position 419 and ΔV_{Mg} was measured. Then, the positively charged MTSET was washed over the channel to completely modify the residue (see Materials and Methods for details). ΔV_{Mg} was measured again in the charge-added channel. Fig. 3 shows the difference in the shift of the conductance with (Fig. 3 *A*) and without (Fig. 3 *C*) MTSET. The modification with MTSET was fast and complete (Fig. 3 *B*). We conclude that introducing a positive charge at position 419 reduces ΔV_{Mg} probably by changing the surface charge density.

These experiments on residue A419C were performed in four different channel backgrounds (WT, F425K, V451K, and F425K/V451K). There was no difference in the effect on

A419C in the four channel backgrounds. Thus, modification of A419C was independent of the charge at the other residues. Fig. 3 *D* shows a summary of the results. The change in ΔV_{Mg} ($\Delta\Delta V_{Mg}$) is robust and close to –2 mV in all channels.

Dissecting the contributions of 425 and 451 to the *Shaker*-to-Kv2.1 conversion

From the section above it is clear that a positive charge at position 419 contributes –2 mV to the −6 mV change in Mg^{2+}-induced shift found for the triple-positive mutation. Here, we will investigate the roles of 425 and 451: Are they dependent of each other? And which is the contribution of each residue? Fig. 4 *A* shows ΔV_{Mg} for different charge combinations. Adding more positive charges reduces the $G(V)$ shift but the contributions of the residues are not equal. In Fig. 4, *B* and *C*, the data are replotted with emphasis on the
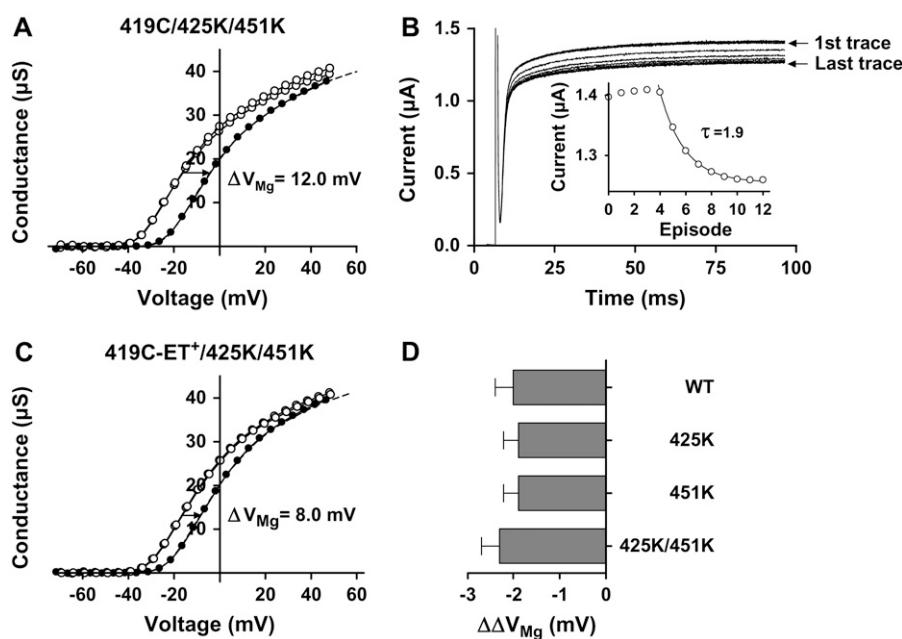
FIGURE 3   The effect of a charge at A419C for Mg^{2+}-induced shifts. The conductance, $G(V)$, of the triple mutation without (*A*) and with (*C*) modification of A419C by MTSET[+] (A419C-ET[+]). Control solution/rinsed oocytes (○) and 20 mM Mg^{2+} solution (●). The dashed lines are control curves shifted along the *x* axis as indicated. (*B*) Modification of 419C with MTSET[+]. MTSET[+] is added to the bath solution at the third trace. The currents were recorded at –10 mV and the time between each trace is 10 s. The current is quickly and irreversibly reduced. (*D*) Summary of change in Mg^{2+}-induced shifts caused by modification of A419C in different channel backgrounds. In all of the mutations the change in ΔV_{Mg} is ∼–2.0 mV.
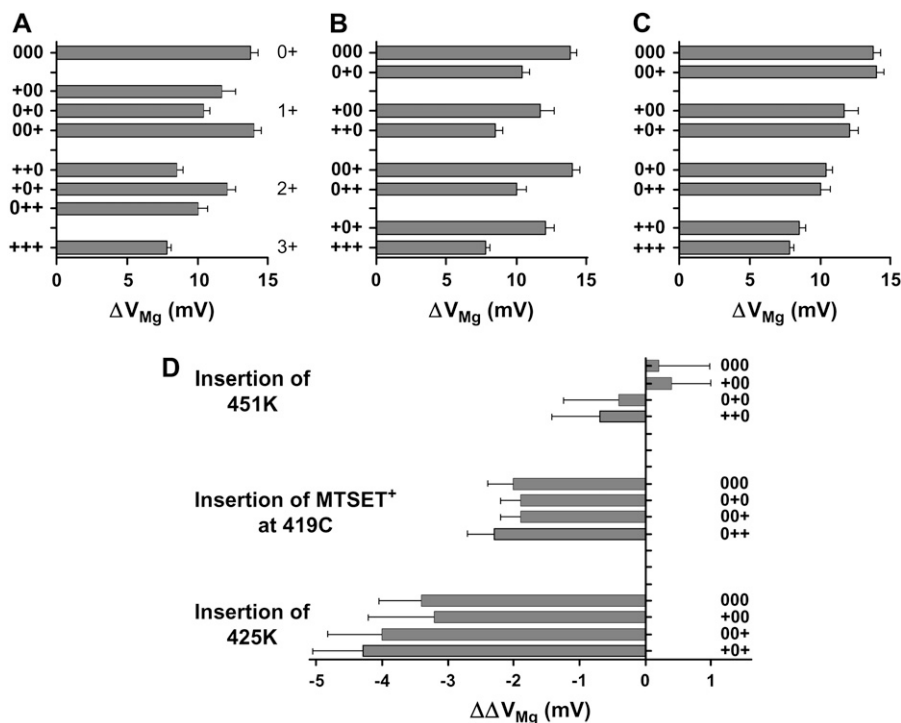
FIGURE 4 Mg^{2+}-induced shifts in eight types of mutated *Shaker* channels. The three-sign code denotes the charges in positions 419-425-451. (*A*) Summary of Mg^{2+}-induced shifts in different mutations. The net charge of the three residues investigated is shown to the right. (*B*) Replot of data from panel *A* with respect to the introduction of a charge in position 425. (*C*) Replot of data from panel *A* with respect to the introduction of a charge in position 451. (*D*) The change in ΔV ($\Delta\Delta V$) for different mutations.

contributions of F425K and V451K, respectively. Fig. 4 *D* shows the difference plot from the data in Fig. 4, *B* and *C*. Two features are obvious. First, there is no large variability depending on the channel background. Thus, the residues are not affecting each other. Second, there is a clear difference in the importance of the different residues. Residue 419 is contributing with, on average, –2.0 mV as shown above. Residue 425 contributes with –3.8 mV, and 451 only with –0.1 mV. Thus, the emerging picture seems to be relatively straightforward: Only two positive charges (at 419 and 425) on the channel surface make the difference between Kv2.1 and the Kv1-type *Shaker* channel with respect to Mg^{2+} sensitivity, and, furthermore, the three investigated charges (at 419, 425, and 451) are independent of each other. In the Introduction we discussed the idea that screenable surface charges also determine the working range of the ion channels with respect to membrane voltage. Charging 419 and 425 (as is done in the A419C-ET$^+$/V451K mutation) not only cut down the Mg^{2+}-induced shift with 5.3 mV, but also shifted the $G(V)$ with $+17$ mV ($V_{1/2}$ shifted from -25 to -8 mV). Thus, the charge valence of position 419 or 425 determines the dynamic range of the channel.

Electrostatic interactions between K427 and F425K are critical for the large effect of 425

In contrast to the clear and internally consistent results regarding the electrostatic effects, the results are unexpected with regard to the proposed positions of the residues and their expected distances to the voltage sensor. In a previous study, we used the Mg^{2+} sensitivity of several residues in the

periphery of the pore domain to map the location of the voltage sensor S4 (5). This mapping was successful and compatible with a series of later experiments (e.g., 21–25), showing the validity of the method. However, the results from 425 are not easy to explain with this structural model. A value of $\Delta\Delta V_{Mg} = -3.8$ mV for 425 suggests that the voltage sensed by the voltage sensor is changed by 14–15 mV (1), corresponding to an electrostatic distance of ~9 Å between 425 and the voltage sensor (9). Even though this distance estimation is based on calculations from much simpler structures than a biomolecule, it seems incompatible with this structural model (25). We suggest three possible explanations for this discrepancy. Either

1. S4 is coming much closer to 425 in the activated state than previously expected;
2. 425 is electrostatically affecting neighboring residues such as the positively charged 427 that then affect the voltage sensor; or
3. The shift effect is mediated via a pore effect (since 425 is close to the pore, the Mg^{2+} effect is indirect via allosteric effect via pore).

Explanation 3 is unlikely because there is no clear sign of current reduction at positive voltages (see Figs. 2 and 3), and explanation 1 is difficult to reconcile with a number of experimental data (13,26). Here, we will explore explanation 2, the electrostatic domino mechanism such as 425 → 427 → voltage sensor.

If 425 is not directly affecting the voltage sensor, it is possible that a charge here affects the position of a neighboring

residue. In the KcsA structure the residues corresponding to 425 (Q58 in KcsA) and 427 (I60) are neutral. If both are positively charged as in Kv2.1 and in our F425K mutations, then they should repel each other and point in different directions. Thus, making 425 positively charged in *Shaker* possibly moves the positive charge of K427 toward the periphery of the pore-forming S5-S6 domain and consequently toward the voltage sensor. To test this hypothesis, we constructed a double mutation (F425C/K427Q). If our hypothesis is correct, the neutralization of 427 to glutamine (Q) should render the channel insensitive to a change of charge at F425C. This is indeed the case: neutralization of 427 to Q shifts the $G(V)$ in negative direction by -7 mV, from -24 mV to -31 mV (Table 1). This indicates that 427 is electrostatically close to the voltage sensor. However, modification of F425C with MTSET when 427 is neutral shows no effect on $V_{1/2}$ or ΔV_{Mg} (Table 1), suggesting that the F425K-to-K427 interaction is critical for the electrostatic profile in the turret. To further investigate this hypothesized interaction we performed molecular dynamics simulation of the turret.

Molecular dynamics

In a first step, we exchanged the KcsA residues in the S5-S6 extracellular loop to *Shaker* residues and performed an equilibration calculation (see Materials and Methods). An extracellular view of one of the four tetramers is shown in Fig. 5 *A*. Notably K427 makes a hydrogen bond with the carbonyl backbone of S421. After the equilibration calculation a positive charge (lysine) is inserted at position 425 instead of the phenylalanine residue. Further calculations show that the hydrogen bond between K427 and the carbonyl in S421 is broken and that K427 swings out to the periphery of the channel (Fig. 5 *B*). The positive charge of K427 now points toward the putative position of S4 (5,21–23,25). Despite the relatively short simulation time (500 ps), K427 in all subunits are changing direction toward the periphery. Thus, the simulation gives a robust illustrative result. To conclude, K425 electrostatically repels K427 out from its interaction with S421 to a new position close to the voltage sensor S4 via an electrostatic domino effect.

The Mg^{2+}-induced $G(V)$ shift strongly correlates with the midpoint of the $G(V)$ curve

The clear results shown above suggest that the three investigated residues (419, 425, and 451) are fixed, inflexible pointlike charges. This implies that the introduction of more and more positive charges not only affects ΔV_{Mg} but should also affect the position of the non-Mg^{2+} affected $G(V)$ curve along the voltage axis. The midpoints of the $G(V)$ curves were measured by fitting the following equation to the experimental data,

$$G(V) = G_{max}/(1 + \exp((V - V_{1/2})/s)), \qquad (2)$$

where G_{max} is the maximum conductance, V is the membrane voltage, $V_{1/2}$ is the midpoint potential, and s is the slope of the curve. $V_{1/2}$ for all mutations are listed in Table 1 and plotted versus ΔV_{Mg} in Fig. 6. The linear correlation is very strong ($r^2 = 0.87$). The slope is -0.29 ± 0.04 and the y axis is crossed at 7 ± 1 mV. This correlation and the absolute values are close to what we have reported for several other Kv channels including several surface mutations (see Fig. 6 in (1)). This fits very well with the surface charge theory and the solution of the Grahame equation (*dashed line*, see (1) for a detailed discussion).

Location of negative surface charges

So far we have focused on the (positive) residues making the difference between *Shaker* and Kv2.1 with respect to ΔV_{Mg}. However, according to the surface charge theory there should be an excess of negative surface charges causing the Mg^{2+}-induced shift (1). Here, we will show data for three possible candidates in the *Shaker* K channel: two in S5-P (E418 and E422) and one in the extracellular S3-S4 loop (D349).

E418 is absolutely conserved in Kv channels and plays an important role for slow inactivation (27). It is located close to the voltage sensor (13) and is thus a good candidate for a functional surface charge. Here we report that removing the negative charge significantly shifts $G(V)$ with $+9$ mV along the voltage axis and significantly reduces ΔV_{Mg} with 1.8 mV (from 13.4 to 11.6 mV) (Table 2). We were not able to change the charge at 418C with MTS reagents because modification almost completely eliminated the current (13).
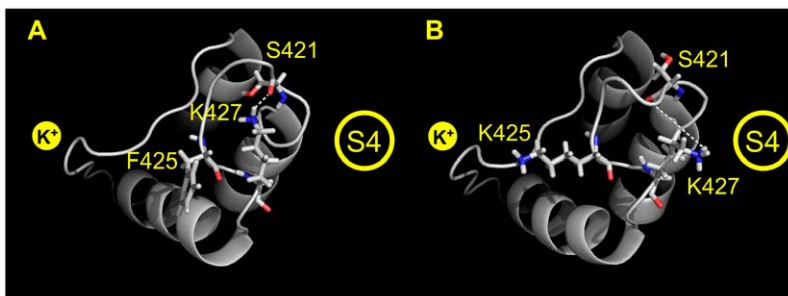

FIGURE 5   Position of K427 in a *Shaker*/KcsA channel. For clarity, only one of four subunits is shown. The K$^+$ ion indicates the ion-conducting pore and S4 indicates the position of the voltage sensor from the neighboring subunit in the Kv1.2 channel (25). (*A*) K427 hydrogen bonds to the carbonyl backbone of S421 in the F425 background. (*B*) K427 points out from the channel pore in the K425 background.
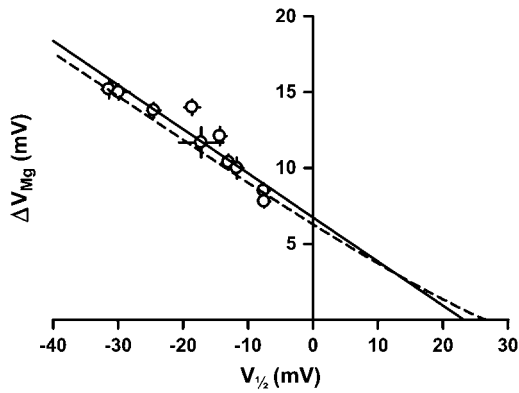
FIGURE 6 ΔV_{Mg} versus midpoint of $G(V)$ curve. Data from the mutations shown in Table 1. Straight continuous line is best fit to data: $y = kx + m$, where $k = -0.29 \pm 0.04$, and $m = 6.7 \pm 0.7$ mV. The x intercept $= 23$ mV. Slope is significantly different from 0 ($p < 0.0001$). The dashed line is a solution to the Grahame equation for the surface charge theory (see (1)).

Application of MTSET$^+$ to 422C significantly shifted $G(V)$ in positive direction along the voltage axis ($+3.0$ mV) and significantly reduced ΔV_{Mg} with 1.1 mV. All these data are quantitatively compatible with a surface charge mechanism (1), suggesting that 418 is closer to the voltage sensor than 422. Application of MTSET$^+$ to 349C significantly reduced ΔV_{Mg} with 1.4 mV. The $G(V)$ curve was not shifted by this application, but this could be explained by nonelectrostatic effects of the $G(V)$, canceling out the electrostatic effect (13).

Thus, the most useful and reliable data, with respect to the surface charge theory, for the investigated residues is $-\Delta\Delta V_{\mathrm{Mg}} = 1.1$ mV for E422C, $-\Delta\Delta V_{\mathrm{Mg}} = 1.4$ mV for D349C and $-\Delta\Delta V_{\mathrm{Mg}} = 1.8$ mV for 418C (measured as ΔV_{Mg} for $WT - \Delta V_{\mathrm{Mg}}$ for E418C). The shifts (or alterations in shifts) can be added because there is an almost linear relationship between surface potential and divalent-cation-induced shifts (Fig. 6 in 1). The total contribution of these residues to ΔV_{Mg} is thus 4.3 mV ($\sim$30% of $\Delta V_{\mathrm{Mg}} = 13.4$ mV for WT).

DISCUSSION

In this investigation, we have succeeded in converting a Mg^{2+}-sensitive Kv1 type *Shaker* channel to a less Mg^{2+}-sensitive Kv2.1 channel with respect to ΔV_{Mg} by swapping three charged residues. Of these residues, 425, located relatively close to the pore, plays the largest role followed by 419 close to the voltage sensor S4. Residue 451 plays a minor role. The electrostatic effects of these residues are independent of each other, but 425 exerts its electrostatic effect via the positively charged residue 427. In parallel, charging 419 and 425 also affects the channel's voltage dependence with 17 mV.

Relation to previous investigations

In several previous investigations we have searched for critical surface charge residues involved in Mg^{2+}- or Sr^{2+}-induced $G(V)$ shifts (1). The main search has been for negative residues, but also positive residues could be important in making the difference between two different channels. In one investigation focusing on the S5-P loop, we assigned residues 418 and 419 to the most important roles, followed by 421 and 422 (9). In later studies, including this one, we showed that 418, 419, and 422 significantly contribute to the electrostatic profile around the voltage sensor S4. However, the surface potential around the *Shaker* voltage sensor should be ~ -40 mV (9) while the negatively charged residues D349, E418, and E422 only contributes with ~ -20 mV. Note that the sum of the neutralization-induced changes in $V_{1/2}$ is $+23.8$ mV, while the sum of the changes in Mg^{2+}-induced shifts (-4.3 mV) multiplied with -3.8 (see Eq. 2 in (1)) is $+16.3$ mV. This suggests we still have not located all surface charges. A possible explanation for this discrepancy is due to backbone dipoles of the peptide chain (not identifiable by mutagenesis). In most proteins, it has been found that the positive end of the peptide dipole points inward toward the center of the protein (28). Consequently, most channel proteins should have a negatively-charged surface due to backbone dipoles that could be the major source for the surface charge effect (1). Also negatively charged phospholipid headgroups could contribute to the negative charge profile. Thus, the critical charges that make the differences between channels could instead be positive residues, such as the one investigated in this study.

In this investigation the single most important residue is 425. The reason we did not find this residue in our previous

TABLE 2 Voltage-dependent parameters for channels with introduced positive charges at negative sites

Channel	$V_{1/2}$ (mV)	$\Delta V_{1/2,\mathrm{MTSET}}$	ΔV_{Mg} (mV)	$\Delta\Delta V_{\mathrm{Mg}}$ (mV)
WT	-23.7 ± 2.2 (13)		13.4 ± 0.3 (11)	
E418C	-15.1 ± 1.0 (14)**		11.6 ± 0.6 (9)*	
E418C-ET$^+$	n.d.	n.d.	n.d.	n.d.
E422C	-17.3 ± 1.8 (8)^{ns}		12.3 ± 0.2 (4)^{ns}	
E422C-ET$^+$	-14.3 ± 2.2 (8)	3.0 ± 0.5 (8)***	11.2 ± 0.1 (4)	-1.1 ± 0.2 (4)*
D349C	-14.9 ± 1.6 (5)*		13.7 ± 0.1 (5)^{ns}	
D349C-ET$^+$	-14.5 ± 1.8 (5)	0.4 ± 0.4 (5)^{ns}	12.3 ± 0.5 (5)	-1.4 ± 0.3 (5)**

$V_{1/2}$ is midpoint of the $G(V)$ curve, $\Delta V_{1/2,\mathrm{MTSET}}$ is the MTSET induced $G(V)$ shift, ΔV_{Mg} is the Mg^{2+}-induced $G(V)$ shift, and $\Delta\Delta V_{\mathrm{Mg}}$ is the MTSET-induced change in Mg^{2+}-induced $G(V)$ shifts. Two-tailed unpaired *t*-test between WT and the mutations ($V_{1/2}$, ΔV_{Mg}). Two-tailed, one sample *t*-test compared to 0 ($\Delta V_{1/2,\mathrm{MTSET}}$, $\Delta\Delta V_{\mathrm{Mg}}$). *ns*, not significant; **, $p < 0.01$; and ***, $p < 0.001$. *n.d.*, not possible to determine.

theoretical consideration (9) was that we assumed independence of the different residues. We here showed that this assumption holds for a residue such as 419, but not for 425, which effect electrostatically depends on the charge of 427.

Structural considerations

For the molecular dynamics calculations we used a *Shaker*-modified KcsA structure. A critical finding is that a positive charge at position 425 electrostatically repels 427 so that 427 swings out from a hydrogen interacting position with the carbonyl backbone of S421 to a more peripheral location closer to the voltage sensor S4 (Fig. 5). The second and the third positive charges in S4 (R365 and R368 in *Shaker*) are very close to the expected position of K427 if the same configuration in Fig. 5 is adopted in the structure of the open Kv1.2 channel. Residue F426, between 425 and 427, is extremely conserved, being a phenylalanine in all eukaryotic Kv channels and a leucine in KcsA. This suggests that this residue makes important hydrophobic interactions with the interior of the channel to keep the turret in place. In the KcsA structure, 59L makes close connections with the absolutely conserved 68W and 83P in the stable aromatic cuff. Our proposed position of K427, closer to S4, fits with previous structural channel models of the S4 position in relation to the pore domain (5,21–23,25).

REFERENCES

1. Elinder, F., and P. Århem. 2003. Metal ion effects on ion channel gating. *Q. Rev. Biophys.* 36:373–427.

2. Frankenhaeuser, B., and A. L. Hodgkin. 1957. The action of calcium on the electrical properties of squid axons. *J. Physiol.* 137:218–244.

3. Hille, B. 2001. Ion Channels of Excitable Membranes, 3rd Ed. Sinauer Associates, Sunderland, MA.

4. McLaughlin, S. 1989. The electrostatic properties of membranes. *Annu. Rev. Biophys. Chem.* 18:113–136.

5. Elinder, F., P. Århem, and H. P. Larsson. 2001. Localization of the extracellular end of the voltage sensor S4 in a potassium channel. *Biophys. J.* 80:1802–1809.

6. Elinder, F., M. Madeja, and P. Århem. 1996. Surface charges of K channels. Effects of strontium on five cloned channels expressed in *Xenopus* oocytes. *J. Gen. Physiol.* 108:325–332.

7. Elinder, F., Y. Liu, and P. Århem. 1998. Divalent cation effects on the *Shaker* K channel suggest a pentapeptide sequence as determinant of functional surface charge density. *J. Membr. Biol.* 165:183–189.

8. Fernandez, D., A. Ghanta, K. I. Kinard, and M. C. Sanguinetti. 2005. Molecular mapping of a site for Cd^{2+}-induced modification of human ether-a-go-go-related gene (hERG) channel activation. *J. Physiol.* 567: 737–755.

9. Elinder, F., and P. Århem. 1999. Role of individual surface charges of voltage-gated K channels. *Biophys. J.* 77:1358–1362.

10. Doyle, D. A., J. M. Cabral, R. A. Pfuetzner, A. Kuo, J. M. Gulbis, S. L. Cohen, B. T. Chait, and R. MacKinnon. 1998. The structure of the potassium channel: molecular basis of K^+ conduction and selectivity. *Science.* 280:69–77.

11. Kamb, A., L. E. Iversen, and M. A. Tanouye. 1987. Molecular characterization of *Shaker*, a *Drosophila* gene that encodes a potassium channel. *Cell.* 50:405–413.

12. Hoshi, T., W. N. Zagotta, and R. W. Aldrich. 1990. Biophysical and molecular mechanisms of *Shaker* potassium channel inactivation. *Science.* 250:533–538.

13. Elinder, F., R. Männikkö, and H. P. Larsson. 2001. S4 charges move close to residues in the pore domain during activation in a K channel. *J. Gen. Physiol.* 118:1–10.

14. DeLano, W. L. 2002. The PyMOL Molecular Graphics System. DeLano Scientific, San Carlos, CA, USA.

15. Cornell, W. D. 1995. A second generation force field for the simulation of proteins, nucleic acids, and organic molecules. *J. Am. Chem. Soc.* 117:5179–5197.

16. Marelius, J., K. Kolmodin, I. Feierberg, and J. Åqvist. 1998. Q: an MD program for free energy calculations and empirical valence bond simulations in biomolecular systems. *J. Mol. Graph. Model.* 16: 213–225.

17. Åqvist, J., and V. Luzhkov. 2000. Ion permeation mechanism of the potassium channel. *Nature.* 404:881–884.

18. Luzhkov, V. B., and J. Åqvist. 2000. A computational study of ion binding and protonation states in the KcsA potassium channel. *Biochim. Biophys. Acta.* 1481:360–370.

19. Luzhkov, V. B., F. Österberg, and J. Åqvist. 2003. Structure-activity relationship for extracellular block of K^+ channels by tetraalkylammonium ions. *FEBS Lett.* 554:159–164.

20. Österberg, F., and J. Åqvist. 2005. Exploring blocker binding to a homology model of the open hERG K^+ channel using docking and molecular dynamics methods. *FEBS Lett.* 579:2939–2944.

21. Broomand, A., H. Männikkö, P. Larsson, and F. Elinder. 2003. Molecular movement of the voltage sensor in a K channel. *J. Gen. Physiol.* 122:741–748.

22. Lainé, M., A. Lin, J. Bannister, W. Silverman, A. Mock, B. Roux, and D. Papazian. 2003. Atomic proximity between S4 segment and pore domain in *Shaker* potassium channels. *Neuron.* 39:467–481.

23. Gandhi, C. S., E. Clark, E. Loots, A. Pralle, and E. Y. Isacoff. 2003. The orientation and molecular movement of a K^+ channel voltage-sensing domain. *Neuron.* 40:515–525.

24. Neale, E. J., D. J. S. Elliott, M. Hunder, and A. Sivaprasadarao. 2003. Evidence for intersubunit interactions between S4 and S5 transmembrane segments of the *Shaker* potassium channel. *J. Biol. Chem.* 278: 29079–29085.

25. Long, S. B., E. B. Campbell, and R. Mackinnon. 2005. Voltage sensor of Kv1.2: structural basis of electromechanical coupling. *Science.* 309: 903–908.

26. Cha, A., G. E. Snyder, P. R. Selvin, and F. Bezanilla. 1999. Atomic scale movement of the voltage-sensing region in a potassium channel measured via spectroscopy. *Nature.* 402:809–813.

27. Larsson, H. P., and F. Elinder. 2000. A conserved glutamate is important for slow inactivation in K^+ channels. *Neuron.* 27:573–583.

28. Gunner, M. R., M. A. Saleh, E. Cross, A. Ud-Doula, and M. Wise. 2000. Backbone dipoles generate positive potentials in all proteins: origins and implications of the effect. *Biophys. J.* 78:1126–1144.